

Observation of Reduced Three-Body Recombination in a Fermionized 1D Bose Gas

B. Laburthe Tolra,* K. M. O'Hara, J. H. Huckans, W. D. Phillips, S. L. Rolston,[†] and J. V. Porto[‡]
National Institute of Standards and Technology, Gaithersburg, MD 20899

(Dated: October 31, 2018)

We investigate correlation properties of a one-dimensional interacting Bose gas by loading a magnetically trapped ⁸⁷Rb Bose-Einstein condensate into a deep two-dimensional optical lattice. We measure the three-body recombination rate for both the BEC in the magnetic trap and the BEC loaded into the optical lattice. The recombination rate coefficient is a factor of seven smaller in the lattice, which we interpret as a reduction in the local three-body correlation function in the 1D case. This is a signature of correlation intermediate between that of the uncorrelated phase coherent 1D mean-field regime and the strongly correlated Tonks-Girardeau regime.

PACS numbers: 39.25+k, 03.67.Lx, 03.75.Lm

The majority of experiments with quantum degenerate gases have been performed in the weakly interacting limit, on Bose-Einstein condensates (BECs) characterized by long-range phase coherence and well described by the mean-field Gross-Pitaevskii (GP) equation [1]. While the success of the GP equation in accounting for many experimental results has been spectacular, it has also led to the search for physics beyond mean-field theory. As in condensed matter physics, there is now great interest in highly correlated systems, where mean-field approaches are inapplicable. Progress toward such correlated systems includes the recent observation of the Mott-insulator transition in BECs loaded into optical lattices [2] and the use of Feshbach resonances to increase interactions between atoms [3]. Here we present evidence of strong correlations in a 1D degenerate Bose gas as reflected in a reduction of three-body recombination.

The role of fluctuations and correlations in Bose gases increases with reduced dimension. In homogeneous systems, BEC is only possible in 3D. In 2D, a Kosterlitz-Thouless transition occurs, and in 1D there is no finite temperature transition [4]. By contrast, BEC is possible in 1, 2 and 3D for trapped systems [5]. Trapped 1D systems with δ -function repulsive interactions are particularly interesting, in that for high density the ground state is a condensate, while in the low density limit the ground state is a highly correlated state known as a Tonks gas [6]. This ground state is an example of “fermionization,” where the repulsive interactions mimic the Pauli exclusion principle. Indeed, the low energy excitation spectrum and the correlation functions are identical to those of non-interacting fermions, and the many-body wave function of the Bose gas is equal to the absolute value of the fermionic wave function [7].

For such a 1D Bose gas, the degree of correlation depends on the ratio between two energies: the repulsive energy of uncorrelated atoms at a given density, $E_{\text{unc}} = gn_{1D}$, and the quantum kinetic energy needed to correlate particles by localizing them with respect to each other on the order of the mean inter-particle distance d , $E_{\text{cor}} = \hbar^2/2md^2$. Here, g is the strength

of the δ -function interaction, m is the atomic mass, and $n_{1D} = 1/d$ is the 1D density. A single parameter $\gamma \equiv E_{\text{unc}}/4E_{\text{cor}} = mg/2n_{1D}\hbar^2$ entirely characterizes a homogeneous 1D gas with repulsive short range interactions. Ref. [6] provides the exact eigenstate solutions for all γ . Recently, these results have been extended to harmonically trapped gases, addressing, *e.g.*, the excitation spectrum [8], the shape of the trapped gas [9], and correlation properties [10].

The many-body ground state has two limiting forms. In the Tonks-Girardeau (TG) regime, where $\gamma \gg 1$, the ground state becomes correlated in order to minimize the interaction energy and the bosons become impenetrable, behaving like fermions as described in [7]. The second and higher-order local correlation functions g_i vanish [11], meaning that no more than one particle can be found at a given position. On the other hand, in the mean-field (MF) regime when $\gamma \ll 1$, the GP equation describes the system well. In this regime the healing length, $l_h = \hbar/\sqrt{mgn_{1D}}$, is much larger than the mean inter-particle distance. Note the counter-intuitive result that the system reaches the correlated regime for *low* 1D densities, contrary to the 3D case where $n_{3D}a_s^3 = (\gamma/2\pi)^3 \gg 1$ corresponds to the correlated regime. (Here a_s is the zero-energy 3D scattering length [16], and γ is the appropriate energy ratio in 3D.)

To probe correlations we measure three-body recombination rates (proportional to the local third-order correlation function g_3) of 1D gases produced in a 2D optical lattice. This technique was used in Ref. [12] to demonstrate that there is a reduction of g_3 in a 3D BEC by a factor of six compared to a thermal gas. We observe a further reduction of three-body recombination in a 1D gas compared to the 3D BEC situation. Even though $\gamma \simeq 0.5$ for our system, which is far from the TG regime, this is a signature that the correlations are significant due to the “fermionization” of the particles.

We realize a 1D gas by confining a 3D gas sufficiently tightly in two directions that the radial confinement energy $\hbar\omega_{\perp}$ is much larger than all other relevant energies in the system: E_{unc} , E_{cor} , $k_B T$, and the axial

trapping energy $\hbar\omega_z$. Since a_s is much smaller than $a_\perp = \sqrt{\hbar/m\omega_\perp}$ ($a_s/a_\perp \simeq 0.1$ in our system), the atom-atom interaction strength is largely determined by a_s , with only a small correction due to confinement [13, 14]: $a_{\text{eff}} = a_s/(1 - 1.46 a_s/\sqrt{2}a_\perp)$. There is no excitation in the radial direction and by integrating over the radial coordinates, one can show [13] that the system is formally equivalent to a true 1D gas with interaction strength $g = 4\hbar^2 a_{\text{eff}}/ma_\perp^2$, so that $\gamma = 2a_{\text{eff}}/(n_{1D}a_\perp^2)$. The 3D density is related to the effective 1D density by $n_{1D} = 1/d = \pi a_\perp^2 n_{3D}$.

Our approach is to load a BEC into the ground state of a deep 2D optical lattice so that the BEC is divided into an array of independent 1D quantum gases, each tubular lattice site acting as a highly anisotropic trap. Our experimental apparatus has been described elsewhere [15]. We achieve BEC with up to $N_0 = 5 \times 10^5$ atoms in the $(F, m_F) = (1, -1)$ hyperfine state of ^{87}Rb (for which $a_s = 5.313$ nm [16]). A Ioffe-Pritchard trap confines the atoms with initial “tight” trap frequencies of $\nu_x = \nu_z = 210$ Hz, and $\nu_y = 8.2$ Hz, giving a peak atomic density of up to 3×10^{14} cm $^{-3}$. Before applying the optical lattice, we adiabatically lower ν_x and ν_z to a “weak” trap frequency of 28 Hz, resulting in peak densities of $\sim 5 \times 10^{13}$ cm $^{-3}$.

We create a 2D optical lattice from two independent, retro-reflected 1D lattices which lie in the xy -plane and intersect at an angle of 80 degrees. The independent 1D lattices are detuned from each another by 5 MHz. All beams derive from a Ti:sapphire laser operating at $\lambda = 810.08$ nm (detuned below both $5S \rightarrow 5P$ transitions at 795 nm and 780 nm), and the polarizations of the lattice beams are in the xy -plane. Each 1D lattice is measured [17] to be $29(1) E_R$ deep (where $E_R = \hbar^2/2m\lambda^2$) [18]. At each lattice site the ground state of the radial motion is well approximated by a gaussian wavefunction with $a_\perp = 58.5(5)$ nm corresponding to an effective $\omega_\perp/2\pi = 33.8(6)$ kHz. By observing dipole oscillations following a sudden, brief displacement of the trap center, we measure the axial frequency along the tubes to be $\omega_z/2\pi = 55.9(6)$ Hz. This frequency results from the combined effect of the magnetic trap and the dipole potential of the lattice beams along the tubes. To load the atoms into the lattice, the laser light is increased over 200 ms with an approximately half gaussian shape (rms width 70 ms), which is adiabatic with respect to all vibrational excitations. We estimate that the interaction-free tunnelling time from one lattice site to the next for a $29 E_R$ lattice is $\simeq 150$ ms. Although this is shorter than the time of the experiment (up to 12 s), it corresponds to an energy much smaller than the interaction energy in the tubes, and should not modify the local 1D correlation properties [19].

To measure the reduction of g_3 due to correlations, we observe the corresponding reduction in the three-body recombination rate coefficient. The local three-body re-

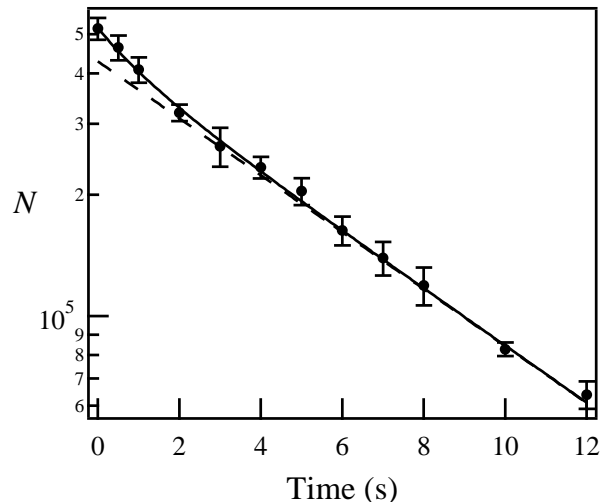


FIG. 1: Number of atoms as a function of time in the 2D lattice. The solid line is a fit to the decay as described in the text, and the dashed line is an extrapolation of the asymptotic 1-body loss.

combination rate (in either 1D or 3D) is proportional to the cube of the local density. For ^{87}Rb , it is known that two-body losses [12, 20], including photoassociation at 810 nm [21], are very small [22]. Our model, therefore, includes only one-body and three-body processes so that the total number of atoms N decays according to

$$\frac{dN}{dt} = -K_1 N - \int K_3^{1D} n_{3D}^3 dV. \quad (1)$$

We account for atomic redistribution during decay through the evolution of the density profile. Determination of the three-body recombination rate coefficient K_3^{1D} requires an accurate estimate of the density, which we ascertain from a measurement of the number of trapped atoms as a function of time, along with a determination of the size and shape of the atom cloud.

Figure 1 shows the total number of atoms as a function of time t in the lattice, obtained by absorption imaging 34 ms after release from the lattice and magnetic trap. We calibrate our absorption measurements by comparing the observed expansion of a released condensate to the known number-dependent expression for the expansion [23]. (The inferred absorption cross section agrees ($\sim 10\%$) with one calculated from the steady state Zeeman sub-level distribution resulting from optical pumping.) The number of atoms in the BEC fluctuates by less than 20% from shot to shot. We automate the experiment to produce a BEC every minute and each data point is typically an average of five measurements. In order to minimize systematic effects due to long term thermal drift of the trap coils, we run current in the magnetic trap *after* the imaging such that the total time that the mag-

netic trap is on is the same for each measurement. While the atoms are in the lattice, we apply a radio frequency shield [20] tuned 500 kHz above the minimum of the trap to reduce heating without significantly increasing the loss of atoms trapped in the lattice.

We measure the size of the lattice-trapped cloud in the xy -plane by phase contrast imaging. The initial column density distribution of the cloud is well described by an integrated Thomas-Fermi (TF) profile, with radii of $R_x = 13.1(5) \mu\text{m}$ and $R_y = 22.5(10) \mu\text{m}$ so that the observed number of atoms per tube at (x, y) is well described by $\mathcal{N}_{\text{tube}} = \mathcal{N}_{\text{max}}(1 - (x/R_x)^2 - (y/R_y)^2)^{3/2}$, where $\mathcal{N}_{\text{max}} = 5N_0\lambda^2/8\pi R_x R_y$ is the number of atoms in the central tube and $\lambda/2$ is the spacing of the tubes. Based on the initial total number and the measured sizes of the cloud, we determine $\mathcal{N}_{\text{max}} = 230(40)$. In the xz -plane, we measure the size of the cloud by absorption imaging. The initial xz density distribution is also described by a TF profile, of radii $R_x = 15(2) \mu\text{m}$ (in agreement with our phase contrast xy -measurement) and $R_z = 17(2) \mu\text{m}$. For our parameters, the atom distribution along the tubes (along z) is not expected to deviate significantly from a TF profile [9]; indeed R_z agrees with the 1D TF value calculated based on \mathcal{N}_{max} . We note that the peak density is $\sim 1 \times 10^{15} \text{ cm}^{-3}$, which would lead to rapid three-body loss in a 3D system.

We observe that the cloud slowly expands in the z -direction over the course of the measurement: the cloud expands by $5 \mu\text{m}$ in 2 s while the R_x and R_y radii remain constant. This expansion is consistent with a 1 kHz/s rate of energy increase, which is less than the expected rate due to spontaneous emission with full equilibration between the radial and longitudinal degrees of freedom, but more than the expected rate with no equilibration. Regardless of the mechanism, this expansion reduces the density only modestly during the first two seconds, when most of the three-body decay occurs. We take this into account empirically in modelling the decay.

To model the decay using Eq. 1, we assume an overall 3D TF density profile with gaussian radial distributions within each tube. In addition, for simplicity of modelling we assume $K_3^{1\text{D}}$ to be a constant (see below). With these approximations, Eq. 1 becomes:

$$\frac{dN}{dt} = -K_1 N - \alpha(t) K_3^{1\text{D}} N^3, \quad (2)$$

where $\alpha(t) = (25/896\pi^4)(\lambda^2/a_{\perp}^2 R_x R_y R_z(t))^2$. The radii R_x and R_y are kept constant at their measured values, and $R_z(t)$ grows linearly in time at the measured rate of $2.5 \mu\text{m/s}$. This differential equation has an analytic solution which gives the total number as a function of time, to which we fit the data of Fig. 1.

With this analysis, we determine $K_3^{1\text{D}} = 1.2(7) \times 10^{-30} \text{ cm}^6 \text{ s}^{-1}$ and $K_1 = 0.16(2) \text{ s}^{-1}$. This result is relatively insensitive to the specific model used for atomic spatial redistribution during decay, and variations among realis-

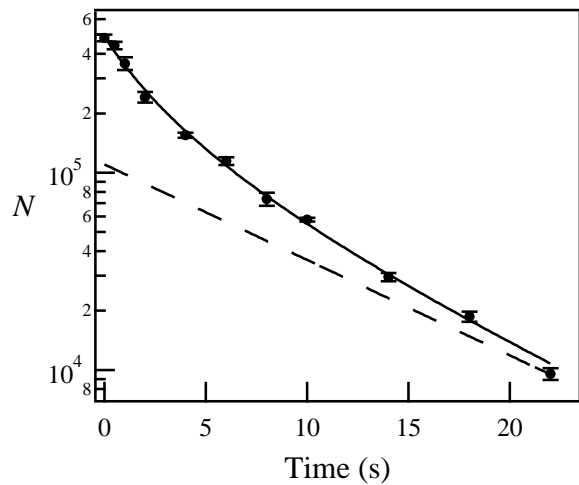


FIG. 2: Number as a function of time in the tight magnetic trap (no 2D lattice). The solid line is a fit to the decay [20], and the dashed line is an extrapolation of the asymptotic 1-body loss.

tic models fall within the quoted uncertainties. We attribute K_1 mainly to optical pumping to states other than the original $(1, -1)$ state, which are untrapped in the combined optical, magnetic and gravitational potential. For the depth and detuning of our lattice, the majority of photon scattering events return the atoms to the original $(1, -1)$ Zeeman sub-level and do not contribute to K_1 . The calculated loss rate for a $29 E_R$ lattice is 0.17 s^{-1} , in good agreement with our measured K_1 .

To determine the reduction of three-body recombination in 1D, we must compare $K_3^{1\text{D}}$ to $K_3^{3\text{D}}$. A comparison in the same apparatus reduces systematic uncertainty due to our 15% number uncertainty. (The effect of this systematic uncertainty is not eliminated entirely because the power law dependence of dN/dt on N is different in 1D and 3D.) We therefore repeat our experiments in a tight magnetic trap in the absence of a lattice, similar to Refs. [12, 20]. (But see [24].) For the $(1, -1)$ state, we measure [25] $K_3^{3\text{D}} = 8.3(20) \times 10^{-30} \text{ cm}^6 \text{ s}^{-1}$ (see Fig. 2), which is in agreement with the value of $5.8(1.9) \times 10^{-30} \text{ cm}^6 \text{ s}^{-1}$ measured in [12].

Comparing our measurements, we find that the ratio of the three-body decay coefficients in 1D and 3D is $0.14(9)$. This represents a factor of seven reduction in $g_3^{1\text{D}}$ over $g_3^{3\text{D}}$, a clear signature of correlations.

For comparison of the observed reduction in g_3 with theory, we calculate γ at the center of each tube. From the experimentally determined density distribution we find at $t = 0$ that $\gamma > 0.34$, with 80% of the atoms having $0.34 < \gamma < 0.65$, and median value $\gamma_m = 0.45$. We do not expect correlations to vary significantly over this range of γ [11], so the assumption of using a single average $K_3^{1\text{D}}$ in the model should be reasonable.

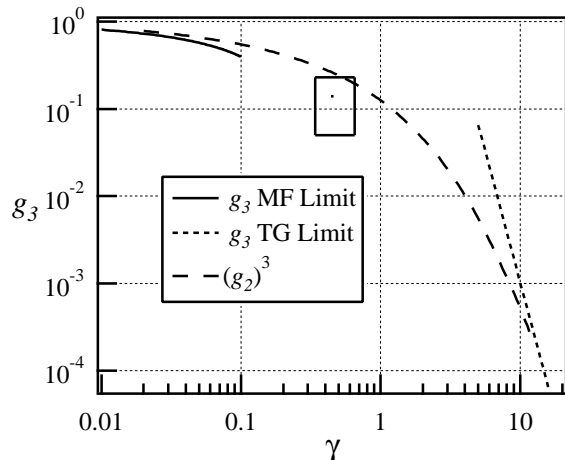


FIG. 3: Comparison of our results with theoretical calculations of the third-order correlation function g_3 vs. γ . The solid and dotted lines represent the MF and TG limits of g_3 from [10], and the dashed line is an estimate [26] of $g_3 = (g_2)^3$, based on g_2 calculated in [11]. The measured suppression factor K_3^{1D}/K_3^{3D} is indicated by the box, where the height represents the measurement uncertainty and the width is the 0% to 80% range of γ for our system.

In Fig. 3 we compare the measured reduction in the three-body loss rate coefficient with theoretical estimates for g_3 in an interacting 1D gas at $T = 0$. There is currently no theory for g_3 in the regime intermediate to the MF and TG limits ($\gamma \simeq 1$). We have plotted an approximate g_3 in the intermediate regime, using the expression $g_3 \simeq (g_2)^3$ [26], and the value of g_2 for a homogenous system from Ref. [11]. The value of g_2 is expected to be insensitive to T for $T \ll T_d \simeq \mathcal{N}_{\max} \hbar \omega_z / k_B$ in this range of γ . From the measured values of \mathcal{N} and ω_z we estimate the distribution of degeneracy temperatures, finding at $t = 0$ a peak value of ~ 13 kHz and a median value of ~ 9 kHz. While it is difficult to measure the temperature in our system, the measured size at $t = 0$ is consistent with zero-temperature TF theory, and is certainly much less than $m\omega_z^2 R_z^2 / 2$, which during the first several seconds does not exceed ~ 6 kHz.

The reduction in K_3^{1D} relative to K_3^{3D} indicates that we are beyond the mean-field regime, and is a signature of the “fermionization” of the bosonic particles in 1D. The fundamental effects of low dimensionality on the correlation properties of a quantum Bose gas are also of practical interest, given the interest in the physics of “atom lasers” loaded in waveguides. In addition, these experiments indicate that high density, strongly correlated 1D systems can be realized without fast decay due to three-body recombination.

We acknowledge helpful conversations with M. Olshanii, G. Shlyapnikov and K. Kheruntsyan, and partial

support from ARDA, ONR and NASA.

* Permanent address: Laboratoire de Physique des Lasers (UMR 7538), Université Paris 13.

† Permanent address: Department of Physics, University of Maryland, College Park, MD.

‡ To whom correspondence should be addressed: trey@nist.gov

- [1] F. Dalfovo, S. Giorgini, L. P. Pitaevskii, and S. Stringari, *Rev. Mod. Phys.* **71**, 463-512 (1999).
- [2] M. Greiner *et al.*, *Nature (London)* **415**, 39 (2002).
- [3] J. L. Roberts *et al.*, *Phys. Rev. Lett.* **86**, 4211 (2001).
- [4] P. C. Hohenberg, *Phys. Rev.* **158**, 383 (1967); J. M. Kosterlitz and D. J. Thouless, *J. Phys. C.* **6** 1181 (1973).
- [5] V. Bagnato, D. Kleppner, *Phys. Rev. A* **44** 7439 (1991); W. Ketterle, N. J. van Druten, *Phys. Rev. A*, **54**, 656 (1996).
- [6] E. H. Lieb and W. Liniger, *Phys. Rev.* **130**, 1605 (1963). E. H. Lieb *ibid.*, p. 1616.
- [7] M. Girardeau, *J. Math. Phys. (N. Y.)* **1**, 516 (1960), *Phys. Rev.* **139**, B500 (1965).
- [8] C. Menotti and S. Stringari, *Phys. Rev. A.* **66**, 043610 (2002).
- [9] V. Dunjko, V. Lorent and M. Olshanii, *Phys. Rev. Lett* **86**, 5413 (2001).
- [10] D. M. Gangardt and G. V. Shlyapnikov, *Phys. Rev. Lett.* **90**, 010401 (2003).
- [11] K. V. Kheruntsyan, D. M. Gangardt, P. D. Drummond, and G. V. Shlyapnikov, *Phys. Rev. Lett.* **91** 040403 (2003).
- [12] E. A. Burt *et al.*, *Phys. Rev. Lett* **79**, 337 (1997).
- [13] M. Olshanii, *Phys. Rev. Lett.* **81**, 938 (1998).
- [14] E. L. Bolda, E. Tiesinga, and P. S. Julienne, *Phys. Rev. A* **68**, 032702 (2003).
- [15] S. Peil *et al.*, *Phys. Rev. A*, **67**, 051603(R) (2003).
- [16] E. G. M. van Kempen, S. J. J. M. F. Kokkelmans, D. J. Heinzen and B. J. Verhaar, *Phys. Rev. Lett* **88**, 093201 (2002).
- [17] We determine the lattice depth by observing the amplitude of diffraction orders following a brief application of the lattice to the BEC, as described in Yu. B. Ovchinnikov, *et. al*, *Phys. Rev. Lett.* **83** 284, (1999).
- [18] All uncertainties reported here are one standard deviation combined statistical and systematic uncertainties.
- [19] P. Pedri and L. Santos, *Phys. Rev. Lett.* **91**, 110401 (2003).
- [20] J. Söding *et al.*, *Appl. Phys. B* **69**, 257 (1999).
- [21] C. Williams, private communication.
- [22] Even though correlations suppress three-body decay more than two-body decay, the upper limit for the two-body decay rate [12] is still negligible.
- [23] Y. Castin and R. Dum, *Phys. Rev. Lett* **77**, 5315 (1996).
- [24] Refs. [12] and [20] used $a_s = 5.45$ nm (E. Burt, priv. commun.) and 5.8 nm, respectively. Using the most recent $a_s = 5.313$ nm reduces their K_3 by 3% and 12%, respectively.
- [25] We also measure the three-body rate for the (2, 2) state, obtaining $K_3^{3D} = 1.5(3) \times 10^{-29}$ cm⁶/s, in agreement with the result $1.8(4) \times 10^{-29}$ cm⁶/s found in [20]. Our

measurements in the (2,2) and (1,-1) states yield a ratio of 1.8(6), confirming that K_3^{3D} is different for these states.

[26] G. V. Shlyapnikov, private communication.